Measurement of Shielding Effectiveness of Electrically-Small Enclosures

Colton R. Dunlap, Christopher L. Holloway, John M. Ladbury,
Joshua A. Gordon, Jason Coder, and Galen Koepke

National Institute of Standards and Technology, 325 Broadway, Boulder, CO, 80305, USA
colton.dunlap@nist.gov, holloway@boulder.nist.gov, and jladbury@nist.gov

Abstract

In the following we propose a technique for determining the shielding effectiveness of an electrically small enclosure with an electrically small aperture. In particular, we use this technique to explore the shielding characteristics of rectangular boxes used to shield devices. Measurement and simulation results are presented in order to validate the technique and to show that, when a source is placed inside the box, different aperture shapes on the face of the enclosure will produce different internal and external field patterns, and have different shielding characteristics.

1. Introduction

The current IEEE 299 standard [1] for determining shielding effectiveness (SE) is limited to the case of physically large, room-size or larger enclosures, which is inadequate for characterizing the shielding of the small enclosures that are used in spaceborne applications. An IEEE 299 Working Group has been formed to investigate different test methods for determining the shielding characteristics of physically small (<1 m on a side), but both electrically small and large enclosures. By electrically small, we mean the largest dimension of the enclosure and apertures, is less than λ/2, λ being the free-space wavelength of the fields generated inside the enclosure. A technique for electrically large, but physical small enclosures was presented in [2]. In this paper we present the following definition for SE for the case of electrically- and physically-small enclosures:

$$SE = 10\log_{10}\left[\frac{TRP_{EN}/V_{EN}^{2}}{TRP_{FS}/V_{FS}^{2}}\right], \quad (1)$$

where TRP_{EN} and TRP_{FS} are the total radiated power of the enclosure with a source in it, and of the some source in free space, respectively. Likewise, V_{EN} and V_{FS} are the voltages applied to the source while it is inside the enclosure and while it is in free space respectively. This differs from how SE is typically defined (see [2]) because the powers are normalized with respect to the voltage used to produce that power. This takes into account any changes in the source impedance that occurs when the source is placed inside of the enclosure. In fact, if the source is indeed an antenna, then the SE can be written as the ratio of the radiation resistance of the antenna in free space to the radiation resistance of the antenna inside the enclosure. In this paper we present both measurement and simulation results, and illustrate the validity of this technique.

2. Plane Wave Analysis

We first analyze the plane-wave response of a box with an aperture in order to understand the associated low-frequency field behavior. The box used in the simulation is a perfect electric conductor version of an actual box with dimensions 86 cm × 74 cm × 42 cm, see Fig. 1(a). The apertures used in this study are the circular, which we compare to the case with the aperture face removed, see Fig. 1(a). The circular apertures used have diameters of 5, 10, and 20 cm. The plane-wave model uses a plane-wave source to generate fields inside the box instead of an internal source.

(a) (b)

Fig 1: (a) Box used in this investigation and (b) spherical dipole used in the measurements.

This approach is important in understanding the results and also invalidates the idea that the fields inside an electrically small enclosure are uniform. In addition, the fields that are scattered into the box from an external source are very similar to those predicted by small-aperture diffraction theory of an aperture on an infinite screen [3, 4].

We compare an analytic model and the simulation in order to get an idea of what the field distribution inside the box will be. First we look at the effects of an incident plane wave polarized parallel to the aperture and incident normal to the aperture. The fields of interest are the scattered waves that are generated in the aperture and travel through to the other region for the infinite sheet analytical model. For the case of an electrically small aperture, the analytic expressions that describe the scattered fields in the area near the aperture simplify to two separate sets of equations: the scattered fields inside of the aperture and those just outside of the aperture. The electric fields inside the aperture are described by [4]:

$$\boldsymbol{E_S} = \frac{-j4k}{3\pi\sqrt{a^2 - x^2 - y^2}} \left[(2a^2 - x^2 - y^2)\boldsymbol{u_x} + (xy)\boldsymbol{u_y}\right] \quad , \tag{2}$$

whereas the scattered electric field that passes to the second region is [3]:

$$\boldsymbol{E_S} = \frac{j2a^3k}{3\pi R^3}\, \boldsymbol{R} \times \boldsymbol{H_0} \quad , \tag{3}$$

where a is the radius of the aperture, $\boldsymbol{R}$ is the observation point, k in the wave-number, and $\boldsymbol{H_0}$ is the magnetic component of the applied electromagnetic field in region 1. Note that equation (2) was derived assuming an X-polarized plane wave with a magnitude of one, which is what is also assumed for our calculations. The interested reader can also find the equations for the scattered magnetic fields in [3] and [4].

The results from the plane-wave numerical models and the aperture on an infinite screen are depicted in Fig. 2. As shown, the scattered fields going through the apertures for both models are very similar. Qualitatively the $|E_x|$ plots show that a dipole polarized in the X direction will have greater coupling to the aperture the closer it is and the more centered it is. The $|E_Y|$ plots are not shown because as expected they are theoretically zero and negligibly small in the simulation. The surprising result is in the Z-polarized field in that it shows that a dipole aligned with the Z-axis will have larger coupling when it is slightly off axis, rather than being in the center.

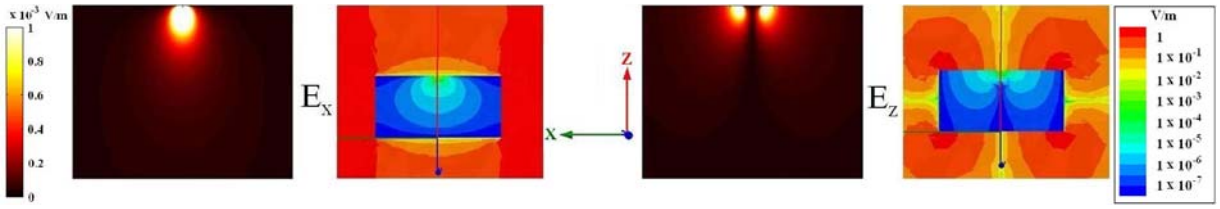

Fig. 2: Z-X slice of the diffracted electric field through a 5 cm circular aperture. The left set of plots are the results from small aperture diffraction theory [3] on an infinite screen. The right set of plots are the numerical model results of the box with a plane-wave incident upon it. In both cases the plane wave is incident along the Z-axis and is polarized along the X-axis. These results are for 10 MHz.

The other numerical plane-wave simulation that has interesting results, but does not have a nice analytic solution, is the case of the wave incident along the X-axis and polarized with the Z-axis. The results for this model are shown in Fig. 3. Again it shows that although the frequency is below the cutoff for modes to exist, the electric field inside the enclosure is not uniform. In this case the Z-polarized field peaks in the center, the X-polarized field has a

peak amplitude off center, and again the Y-polarized field is very small. It is quite clear from these models that any technique used to characterize the shielding of the enclosure requires many measurements with the internal source placed in different locations and orientations. Other apertures are investigated in [5]. Measurements for two orientation of an internal source are given next.

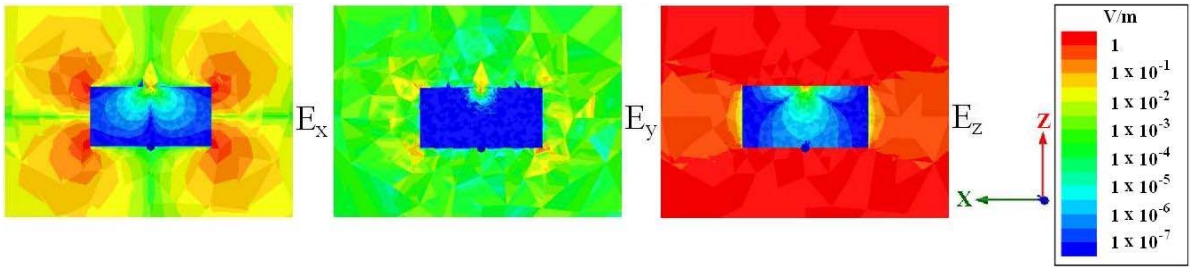

Fig. 3: Numerical model results of a plane wave polarized in the Z-axis and incident along the X-axis for 10 MHz.

3. Shielding Effectiveness

In order to numerically calculate the SE of the above box (see Fig. 1(a)), a 10 cm linear dipole inside the box is used as a source in the simulation. The total radiated for a dipole in free-space and the total radiated power for the dipole placed inside the box were calculated. The driving voltage for the dipole was held constant for these two cases. With the numerically obtained total radiated and the driving voltage, equation (1) is used to obtain the SE. These numerical calculated SE data are shown in Figs. 4 and 5.

A special type of antenna is required to control the driving point voltage during a test. In the measurements presented here we use a commercially made 10 cm spherical dipole that was originally developed at the National Institute of Standards and Technology (NIST), see Fig 1(b). This spherical dipole takes an input signal that sets the voltage across a 200 Ω resistor. By keeping the signal power level constant the voltage remains constant. Also, the feed cable for this antenna is a fiber optic cable, which means that low frequency energy will not couple to it and cause error in the measurements. We preformed measurements in both a reverberation chamber and in a transverse electromagnetic (TEM) cell. The reverberation chamber measurements, performed for the frequencies 100 MHz to 200 MHz, measure total radiated power, which directly corresponds to the numerical models. On the other hand, the TEM cell is just a transmission line and, as such, the energy that is measured is the mode generated by the source that couples to the septum. It was initially unknown whether these measurements would have any correspondence with the numerical model and reverberation chamber, but the TEM cell provides a very compact measurement facility for making these sorts of measurements down to 10 MHz. Thus, for each orientation of the dipole inside the box, the entire structure is placed in various orientations inside the TEM cell. Once the measurements are taken there are two methods that can be used that produce similar results (within a couple of decibels): a worst case approach and an averaging approach. In the worst case approach the orientation that has the largest coupling to the TEM cell is used to calculate the SE. In the averaging approach the different measurements are averaged together to obtain the SE.

The measurement results that correspond to the open box and circular aperture are shown in Fig. 4 and are compared with the numerical modeling results. These results are for the axis of the dipole pointing at the aperture. Fig. 5 shows the same comparisons except that the dipole is aligned parallel to the aperture. As can be seen in the plots the different methods give strikingly similar SE results across the frequency band. Note that, at and above 50 MHz, the TEM cell data have resonant effects that are caused by the interaction of the test article and the cell. At frequencies ranging from 100 MHz to 200 MHz both the TEM cell and the reverberation chamber give SE values that are very similar. The main difference between the two measurements is that the test facilities have different resonant effects at these frequencies. When comparing the measurement results to those obtained from the simulations the similarities are remarkable. The uncertainties in these measurements are estimated to be 5 dB - 10 dB and a detailed discussion is found in [5].

4. Conclusion

In this paper, we have proposed a technique for determining the SE for electrically-small and physically-small enclosures. The approach consists of placing a voltage-controlled dipole inside the testing enclosure, and measuring the TRP and the associated drive voltage. Using the same drive voltage, which requires an increase in drive power, the TRP is again measured with the active dipole inside the test article. By having the same drive voltage the ratio TRP_{EN}/TRP_{FS}

will give a value for SE in which the impedance mismatch terms have been canceled. In order to compare this approach, we presented data from two test facilities (a reverberation chamber and a TEM cell), numerical simulations, and diffraction theory of an electrically small aperture on an infinite conducting screen. The comparison illustrates the validity of the proposed approach. More details on this approach and other comparisons are given in [5].

5. References

[1] *IEEE Standard Method for Measuring the Effectiveness of Electromagnetic Shielding Enclosures,* IEEE Standard 299, 1997 .

[2] C. L. Holloway, D. A. Hill, M. Sandroni, J. M. Ladbury, J. Coder, G. Koepke, A. C. Marvin, and Y. He, "Use of Reverberation Chambers to Determine the Shielding Effectiveness of Physically Small, Electrically Large Enclosures and Cavities," *IEEE Trans. Electromagn . Compat.*, vol. 50, no. 4, pp. 770-782, November 2008 .

[3] V. V. Klimov, and V. S. Letokhov, "A Simple Theory of the Near Field in Diffraction by a Round Aperture," *Optics Communications* 106, pp. 151-154, 1994

[4] C. J. Bouwkamp, "On Bethe's Theory of Diffraction by Small Holes," *Philips Res. Rep.* 5, pp. 321-332, 1950.

[5] C. R. Dunlap, C.L. Holloway, J. M. Ladbury, J. Gordon, J. Coder, and G. Koepke, "Shielding Effectiveness of Physically Small, and Electrically Small Enclosures and Cavities," in preparation for *IEEE Trans. Electromagn . Compat.*.

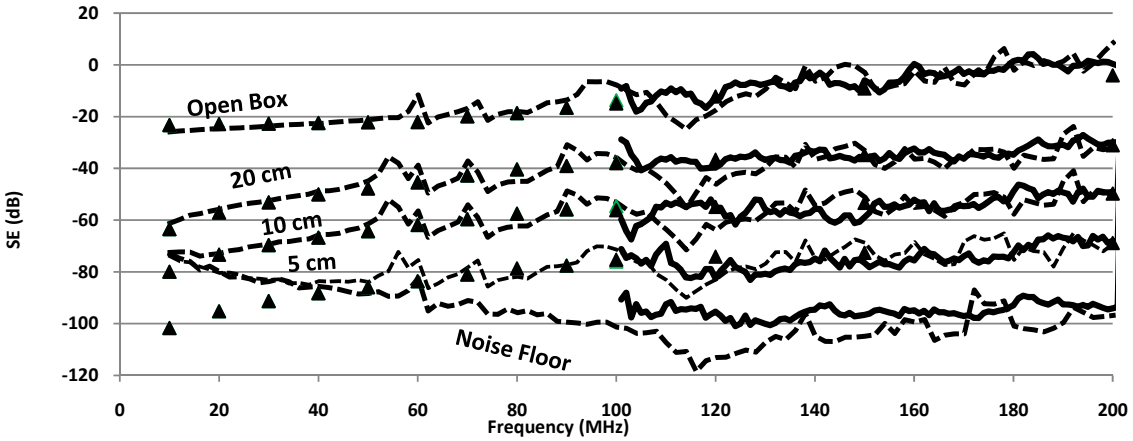

Fig. 4: SE comparison between the TEM cell (dashed), reverberation chamber (solid), and numerical model (triangles) for the open box and circular apertures with dipole pointing at the aperture. The noise floor is for both the TEM cell and reverberation chamber setup.

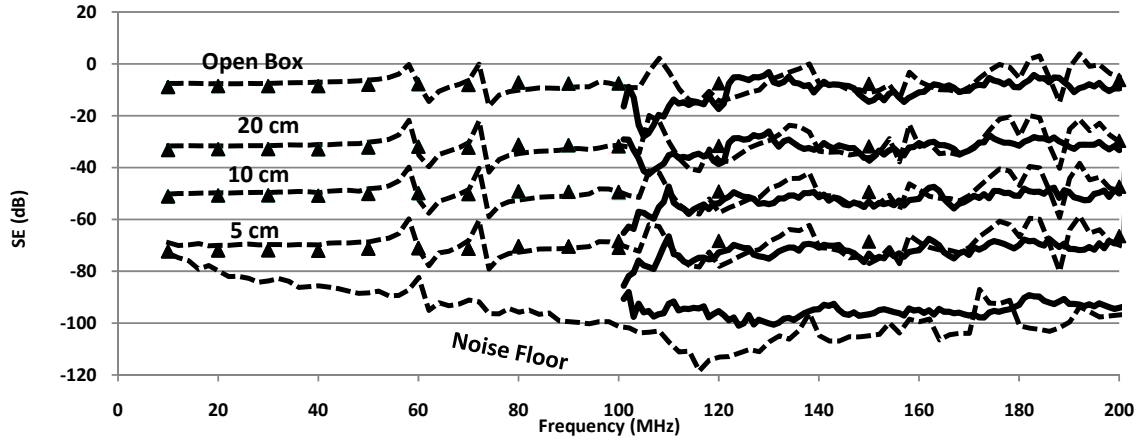

Fig. 5: Same as Fig. 4, except now the open box and circular aperture orientations are parallel to the dipole axis. The noise floor is for both the TEM cell and reverberation chamber setup.